Available online at www.sciencedirect.com
SCIENCE DIRECT®
Journal of Power Sources 142 (2005) 382–388
JOURNAL OF POWER SOURCES
www.elsevier.com/locate/jpowsour

Electrochemical characterization of electrospun activated carbon nanofibres as an electrode in supercapacitors

Chan Kim

Faculty of Applied Chemical Engineering, Chonnam National University, Gwangju 500-757, Republic of Korea

Received 3 August 2004; accepted 6 November 2004
Available online 1 January 2005

Abstract

A new form of nanofibre web electrode has been fabricated for a supercapacitor using electrospun polybenzimidazol (PBI)-based activated carbon nanofibres. A PBI solution in dimethyl acetamide (DMAc) is electrospun to a fibre web that consists of 250 nm ultra-fine fibres. The web is successfully activated by steam of 30 vol.% and the specific surface area of the activated web is in the range of 500–1220 $m^2 g^{-1}$. The electrochemical properties of electrodes and the capacitive behaviour of the resulting capacitors are systematically studied using cyclic voltammetry, ac impedance and constant-current discharge tests. The specific capacitance ranges from 35 to 202 $F g^{-1}$, depending on the activation temperature. The nanofibre web activated at 800 °C exhibits the largest specific surface area and results in the highest capacitance. The capacitance of the electrical double-layer capacitor is strongly dependent on the specific surface area, pore volume, and resistivity of the samples.

Keywords: Electrospinning; Activated carbon nanofibre; Supercapacitor; Specific surface area; Specific capacitance

1. Introduction

Though various materials have been examined supercapacitors [1–6] the application is still limited in terms of specific energy. Recently, in order to enhance the specific energy and power of supercapacitors, many researchers have put much effort into the development and modification of carbonaceous materials, such as controlling the pore size distribution, introducing electroactive metallic particles or electroconducting polymers and fabricating hybrid-type cells [7–9]. Various forms of carbonaceous materials, i.e., powder [10], fibre, paper (fabric or web) [5], carbon nanotubes and the related nanocomposites [2,6,11] are candidates for becoming electrodes of supercapacitors.

Electrospinning is a method of producing nanofibres by using an electrostatic repulsive force and an electric field between two electrodes, by applying high voltage to a polymer solution or a melt, so that it can produce a web of nanofibres [12–14]. The nano-size diameters result in a high specific surface area. Therefore, there have been intensive studies on the electrospinning of polymer solutions so as to take advantage of a fast, simple, and relatively inexpensive process. A web consisting of activated carbon fibres would be particularly useful for the electrodes of supercapacitors with certain advantages pertaining to the unnecessary process of additions to the binder, which normally reduce electrical conductivity and lead to degradation of the performance of the supercapacitors.

Recently, carbon nanofibre webs have been prepared [6] through the electrospinning technique and offer the prospect of accelerating the application of these materials in electrical energy-storage systems. Polybenzimidazol (PBI) is a particularly good candidate for producing such webs as the carbon nanofibres exhibit excellent thermal stability, are durable to chemicals, have high mechanical strength, and give a high carbon yield. Although precursors of carbon fibres such as cellulose, PAN (polyacrylonitrile), phenol resin and pitch required a stabilization process prior to carbonization or activa-

E-mail address: ckim37@empal.com.

0378-7753/$ – see front matter © 2004 Elsevier B.V. All rights reserved.
doi:10.1016/j.jpowsour.2004.11.013

tion to sustain the original shape at the carbonization temperature, the PBI-based electrospun fibre does not require stabilization because of its thermosetting property that originates from the high rigidity of the polymer chains. The stabilization step is the rate-determining step of the overall manufacturing processes, and is very costly. Therefore, since the PBI-based electrospun fibre can be easily used for carbon and activated carbon fibres with carbonization and/or activation without further treatment, they should provide a high carbon yield and energy savings.

The work evaluates a PBI-based activated carbon nanofibre web as a novel electrode material for electric double-layer supercapacitors. The webs consist of homogeneously distributed nanofibres with a diameter of about 250 nm. The specific surface area of the web is controlled by varying the activation conditions.

2. Experimental

2.1. Electrospinning

A solution of 20 wt.% PBI in dimethyl acetamide (DMAc) was gently stirred for 4 h at about 185 °C. Evaporative losses of the solvent during dissolution were avoided by refluxing the evaporated solvent. The solution was spun into a fibre web by means of an electrospinning apparatus equipped with power supply (NT-PS-35K, NTSEE Co., Korea). The polymer solution was placed in a 20 cm^3 syringe with a capillary tip of 0.5 mm in diameter. The positive terminal of the high-voltage power supply was clamped to the syringe tip and the negative was connected to a metal collector. The electrospun fibre was collected on aluminum foil that was wrapped on a metal drum rotating at approximately 300 rpm.

Nanofibre webs were heated to 700, 750, 800 or 850 °C at a heating rate of 5 °C min^{-1} in a flow of nitrogen. The webs were activated by supplying a volume of 30% steam in a carrier gas of nitrogen for 30 min at the given temperature.

The electrospun and activated carbon nanofibres (ACNF) were examined with a scanning electron microscope (SEM, Hitachi, S-4700, Japan). The specific surface area and pore-size distribution were evaluated by using the Brunauer–Emmett–Teller (BET) equations after preheating the ACNF at 423 K for 2 h under vacuum.

2.2. Electrochemical testing

The electrical conductivities along the winding direction of the webs were measured by the four-point probe method (Model 3387-11, Kotronix, Japan). The cross-sectional area of the web, A, was calculated by multiplying the measured width by the measured thickness of the sample web. Then, the electrical conductivity, σ, was calculated according to:

$$\sigma = \frac{L}{AR} \tag{1}$$

where R is the electrical resistance in Ω; A the cross-sectional area in cm^2; L the distance between the electrode positions in cm.

Supercapacitor cells were built by assembling two 2.25 cm^2 ACNF electrodes with a polypropylene separator (Cellgard 3501, 25 μm). A glassy carbon plate was then attached on each side to collect currents on the surface of the ACNF electrodes. The electrode performances were measured in 1 M H_2SO_4 at 25 °C. The capacitance of the electrodes was galvanostatically measured with a WBCS 3000 battery cycler system (WonA Tech Co., Korea) in the potential range of 0–0.9 V and at a current density of 1–10 mA cm^{-2}. The cell capacitance was calculated from the slope of the discharge, i.e., on the basis of Eq. (2):

$$C = i\left(\frac{\Delta t}{\Delta V}\right) \tag{2}$$

where C is the capacitance of the cell in farads; i the discharge current in amperes; Δt the discharging time from 0.54 to 0.45 V (about 60–50% of the initial potential); ΔV the potential variation in the time range measured, i.e., the slope in volts per second (V s^{-1}). In a symmetrical system, the specific capacitance C_m in farads per gram of samples (F g^{-1}) is related to the capacitance of the cell C:

$$C_m = \frac{2C}{m} \tag{3}$$

where m is the weight (g) per electrode.

Cyclic voltammetry of the unit cell was performed in the potential range of 0–0.9 V with scan rates from 1 to 500 mV s^{-1}. The capacitance, C, is calculated from the CV for a two-electrode system according to:

$$C = \int i\frac{\mathrm{d}t}{\mathrm{d}v} \tag{4}$$

where i is the current; t the time; v the voltage.

The ac impedance measurement of the unit cell was performed in the frequency range of 100 kHz to 10 mHz by using an electrochemical impedance analyzer (Jahner Electrik IM6, Germany).

3. Results and discussion

3.1. Preparation and morphology of activated carbon nanofibre webs by electrospinning

A schematic diagram of the electrospinning apparatus and scanning electron micrographs of the electrospun PBI nanofibre web at low and high magnification are presented in Fig. 1. The fibre diameter lies in the distribution range of 100–500 nm, with an average of 250 nm. The nanofibres were partially aligned along the winding direction of the drum winder.

The diameter distribution percentage of the fibres slightly decreased with an increase in activation temperature (Fig. 2).

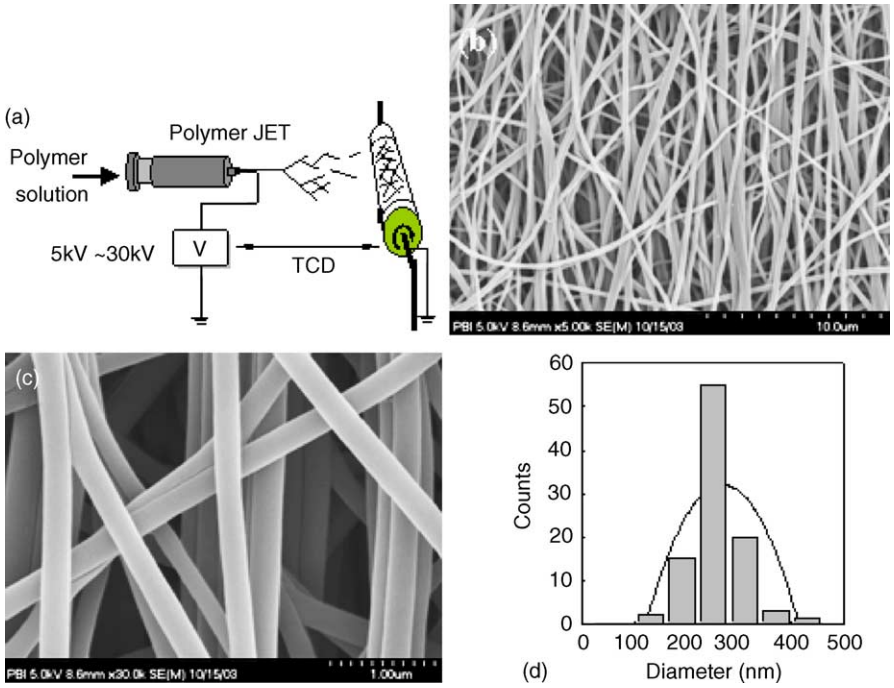

Fig. 1. (a) Schematic diagram of electrospinning apparatus, electron micrographs of electrospun PBI nanofibre web, (b) low magnification, (c) high magnification. The histogram (d) displays the statistical distribution of nanofibre diameters, which show an average diameter at 250 nm (spinning conditions: concentration—20 wt.%, applied voltage—20 kV, tip to collector distance (TCD)—15 cm).

Generally, the fibre diameter should not be decreased by steam activation. In the activation condition used here, however, the nanofibre webs were heated to 700 and 850 °C and then the activation process started. Thus, the decrease in fibre diameter is due to the more severe carbonization at higher temperatures.

The effect of pore rearrangement on the adsorption properties of PBI-based activated carbon nanofibres was inves-

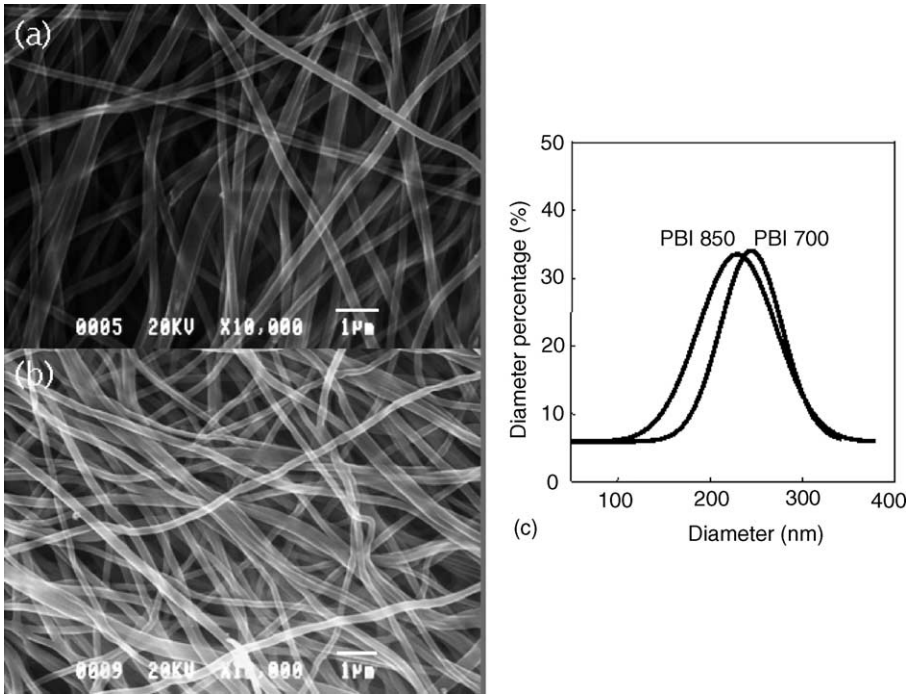

Fig. 2. Electron micrographs of PBI-based activated carbon nanofibres with activation temperatures of (a) 700 and (b) 850 °C. The fibre diameter distribution percentage (calculated from the micrographs) is given in (c).

Table 1
Surface characterization of PBI-based activated carbon nanofibres

Activation temperature (°C)	Activation yield (%)	Specific resistivity (Ω cm)	BET S.S.A.[a] ($m^2\ g^{-1}$)	V_{meso}[b] ($ml\ g^{-1}$)	V_{micro}[c] ($ml\ g^{-1}$)	W_{micro}[d] (nm)
700	59	174	500	0.06	0.28	0.63
750	55	8	660	0.12	0.39	0.64
800	49	2	1220	0.20	0.71	0.64
850	40	0.15	810	0.25	0.47	0.66

[a] Specific surface area calculated by BET method.
[b] Mesopore (1.7–300 nm) volume calculated with Barret, Joyner and Halenda (BJH) method based on the Kelvin equation.
[c] Micropore volume calculated with Horvath–Kawazoe (HK) method.
[d] Average micropore width calculated with HK method.

tigated by nitrogen adsorption measurements at 77 K. The porosity parameters of the samples under study are summarized in Table 1. The pore volume, and BET specific surface areas appear to increase with increasing activation temperature between 700 and 800 °C. On the other hand, at the highest activation temperature of 850 °C, there is a decrease in BET specific surface area. Obtaining the highest BET surface area and pore volume with the sample activated at the optimum temperature is a normal, but not an entirely opposite, trend compared with conventional activated carbon fibre. Because the PBI-based activated carbon nanofibre is very fine, the specific surface area is thought to decrease by unification of the micropores rather than by creation of more micropores at the fibre surface at elevated activation temperatures between 800 and 850 °C [16].

3.2. Electrical conductivity of activation carbon nanofibre webs

The electrical conductivity of the activated carbon nanofibre web as a function of activated temperature is shown in Fig. 3. The electrical conductivity increases with increasing activation temperature namely, 5.8×10^{-3} and 6.7 S cm^{-1} at 700 and 850 °C, respectively. In specific terms, the electrical conductivity is increased by about three orders of magnitude. The reason is that the nanofibre material activated at higher temperatures is promoted spontaneously by both carbonization and activation.

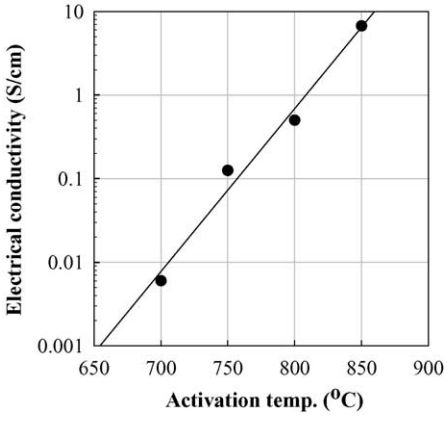

Fig. 3. Electrical conductivities of activated PBI webs as a function of activation temperature.

3.3. Cyclic voltammetry

The electrochemical properties of activated carbon nanofibre web electrodes were studied by cyclic voltammetry in a 1 M H_2SO_4 aqueous solution. Typical cyclic voltammograms (CVs) of the capacitor cells at different scan rates are shown in Fig. 4. The data demonstrate that the electrodes are stable within the potential range employed, and that peaks due to faradic current are not observed for the capacitor cells. The voltammograms also show that the induced current increases according to the activation temperature. When the activation temperature is increased from 700 to 850 °C, the *CV* curve approaches a rectangular shape, which indicates not only a reduction in the ESR (equivalent series resistance) of the nanofibre web electrode, but also a reduction in the hindrance to the motion of ions in the pores.

The specific capacitance as a function of the sweep rate for the samples activated at various temperatures is given in Fig. 5. In general, the specific capacitance decreases gradually with increasing potential sweep rate. Ions that are larger than the pore size may block the entrances of the micropores and thus reduce the specific capacitance. For samples activated at 700 °C, the specific capacitance at a sweep rate of 500 mV s^{-1} is reduced by about 96% compared with the specific capacitance at 1 mV s^{-1}, as shown in Fig. 5(a). For the electrode activated at 800 °C, however, the capacitance reduced by only about 34% even at high sweep rates (Fig. 5(c)). The specific capacitance of PBI-based electrodes activated at 750, 800 and 850 °C exhibit a similar performance over the whole range of sweep rates; the electrode activated at 800 °C performed better than that activated at 850 °C. The larger drop in capacitance at low activation temperatures indicates that more internal resistance has occurred. The behaviour can be explained by the accessibility of ions on the pore surface. The electrodes activated at 750, 800 and 850 °C have a specific surface area above 600 $m^2\ g^{-1}$ and the specific resistivity is the lowest for the electrode activated at 850 °C. Consequently, the electrode with larger BET surface area and lower resistivity will give a higher specific capacitance at a higher sweep rate. This high capacitance sug-

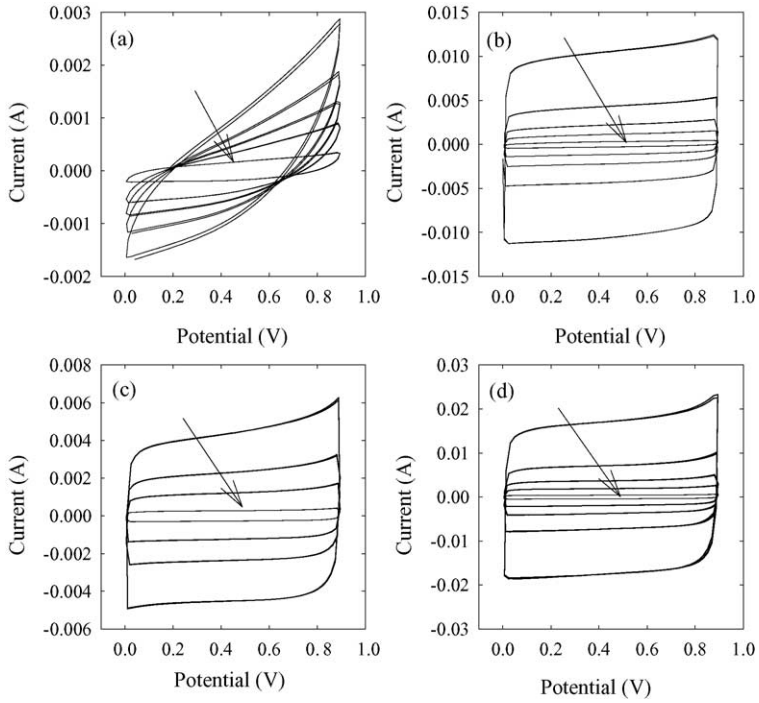

Fig. 4. Cyclic voltammograms of activated carbon nanofibre web electrodes (2.25 cm^2) in 1 M H_2SO_4 at various sweep rates. Arrow indicates voltammograms at decreasing sweep rates (from 500 to 1 mV s^{-1}). Activation temperatures: (a) 700 °C; (b) 750 °C; (c) 800 °C; (d) 850 °C.

gests a certain practical importance for applications of various devices.

3.4. Constant charge–discharge testing

Typical charge–discharge curves of samples in the 1 M H_2SO_4 solution at a constant current density of 1 mA cm^{-2} are given in Fig. 6. It can be seen that nanofibre web electrodes with a large BET specific surface area exhibit a longer discharging interval, which indicates a higher electrical capacity for there samples. Based on the results of charge–discharge cycling, the specific discharge capacitances of the samples were calculated according to Eqs. (2) and (3). The results are shown in Fig. 7.

The curves are almost linear and the sudden drop in potential at the beginning of charge and discharge is associated with the ohmic resistance of the cell [15]. The capacitance gradually decreases with increase in discharge current density. This behaviour is remarkable for microporous carbons. At the lowest discharge current density of 1 mA cm^{-2}, the specific capacitance of the sample activation temperature for 700, 750, 800 and 850 °C is about 36, 180, 202 and 194 F g^{-1}, respectively. The specific capacitance of the latter three sam-

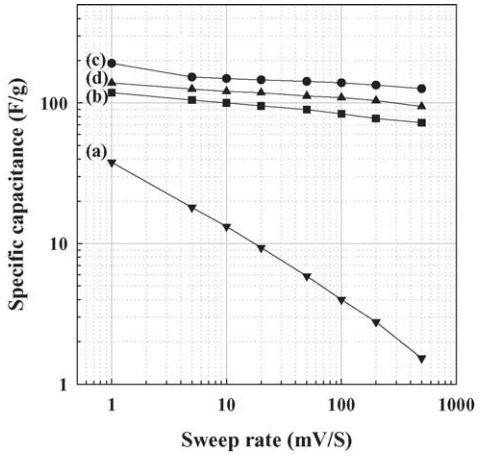

Fig. 5. Dependence of specific capacitance on sweep rate for samples at various activation temperatures: (a) 700 °C; (b) 750 °C; (c) 800 °C; (d) 850 °C.

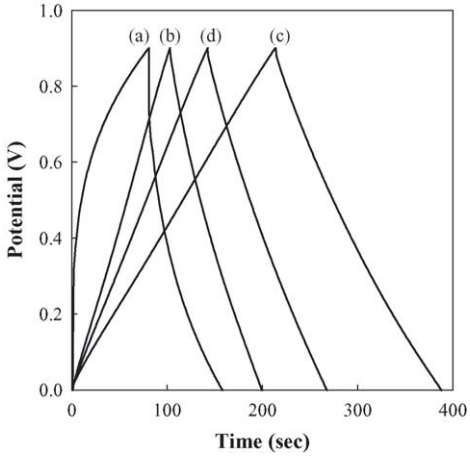

Fig. 6. Typical charge–discharge curves of PBI-based electrodes as function of activation temperature: (a) 700 °C; (b) 750 °C; (c) 800 °C; (d) 850 °C. Charge–discharge current density at 1 mA cm^{-2}.

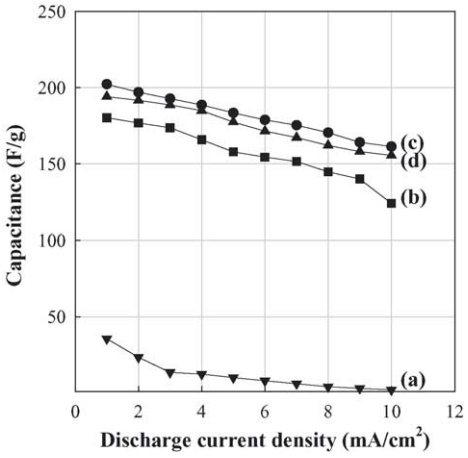

Fig. 7. Dependence of specific capacitance on discharge current density for PBI-based activated carbon nanofibre web electrodes (2.25 cm^2) as a function of activation temperature: (a) 700 °C; (b) 750 °C; (c) 800 °C; (d) 850 °C.

ples is similar at all discharge current densities. These results are very consistent with Fig. 5.

3.5. The ac impedance testing

In general, the resistance in an electrochemical capacitor has electronic and ionic contributions. The ionic contributions include the separator resistance and that due to ion conduction in electrolyte in the electrode pores [16]. The electronic contributions include the bulk resistivity of the electrode material, i.e., particle–particle contacts, particle–current–collector contacts, the bulk current–collector, and external wires. The technique of ac impedance spectroscopy, which distinguishes the resistance and capacitance of devices, was employed to analyze the performance of the capacitor cells. The impedance spectra of these cells are shown in Fig. 8. The frequency ranged from 10 mHz to 100 kHz. The ideally polarizable capacitance will give rise to a straight line along the imaginary axis. In a real capacitor with a series resistance, this line has a finite slope that represents the diffusive resistivity of the electrolyte within the pores of the electrode. The diffusive line of the nanofibre web electrode becomes closer to an ideally straight line with increase in activation temperature. An increase from 700 to 850 °C reduces the resistance of the sample by three orders of magnitude and widens the pores as indicated by the data given in Table 1.

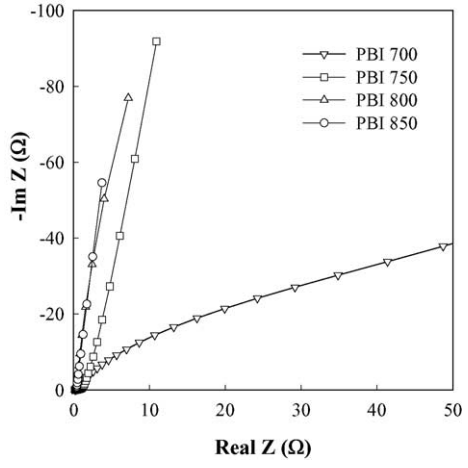

Fig. 8. Complex-plane impedance plots of PBI-based activated carbon nanofibre web electrodes with various activation temperatures (ac signal level = 10 mV; frequency range = 10 mHz to 100 kHz).

The formation of abundant micropores and mesopores may also enhance the diffusivity of the hydrated ions in the pores, and consequently reduce the resistance of the nanofibre web electrode. The enhanced conductivity and enlarged pore openings would contribute to the reduction in cell resistance representing the sum of the bulk and electrode–solution interfacial resistances from the separator, the electrode itself, the contact between the component fibres, and ion transfer in the pores. Lowering the resistance would increase current density on the surface of electrode and lead to an enhancement of the diffusion rate of the ions toward the electrode. This, in turn, results in a high specific capacitance, particularly at high current density.

4. Conclusion

A 20 wt.% PBI solution has been successfully electrospun into yellow coloured webs that consist of fibres with diameters of 250 nm. The PBI web has been activated with a yield of about 40% and with maintaining the original shape of the individual fibres. The specific surface areas of activated carbon nanofibres are in the range of 500–1220 $m^2\ g^{-1}$. The surface area increases and decreases with increasing activation temperature.

Nanofibre webs activated at 800 °C exhibits the highest capacitance and the largest specific surface area. The characteristics appear to be correlated with the vertical slope of the impedance plot with no charge transfer resistance. It is proposed that the capacitor performances are strongly dependent on the charge resistance and surface area. These parameters deliver the majority of stored energy.

Acknowledgements

Support for this work was provided by KOSEF under grant number R01-2003-000-10100-0.

References

[1] R. Kötz, M. Carlen, M. Electrochim. Acta 45 (2000) 2483.
[2] K.H. An, W.S. Kim, Y.S. Park, J.M. Moon, D.J. Bae, S.C. Lim, Y.S. Lee, Y.H. Lee, Adv. Funct. Mater. 11 (2001) 387.
[3] S.T. Mayer, R.W. Pekala, J.L. Kaschmitter, J. Electrochem. Soc. 140 (1993) 446.
[4] A. Yoshida, S. Nonaka, I. Aoki, A. Nishino, J. Power Sources 60 (1996) 213.

[5] S.R. Hwang, H. Teng, J. Electrochem. Soc. 149 (2002) 591.
[6] C. Kim, K.S. Yang, Appl. Phys. Lett. 83 (2002) 1216.
[7] K. Jurewicz, S. Delpeux, V. Bertagna, F. Beguin, E. Frackowiak, Chem. Phys. Lett. 347 (2001) 36.
[8] E. Frackowiak, F. Beguin, Carbon 39 (2001) 937.
[9] J.P. Zheng, P.J. Cygan, T.R. Jow, J. Electrochem. Soc. 142 (1995) 2699.
[10] M. Endo, Y.J. Kim, T. Maeda, K. Koshiba, K. Katayama, M.S. Dresselhaus, J. Mater. Res. 16 (2001) 3402.
[11] M. Hughes, Z. Chen, M.S.P. Shaffer, D.J. Fray, A.H. Windle, Chem. Mater. 14 (2002) 1610.
[12] J.M. Deitzel, J. Kleinmeyer, D. Harris, N.C.T. Beck, Polymer 42 (2001) 261.
[13] H. Fong, D.H. Reneker, I. Chun, Polymer 40 (1999) 4585.
[14] I.D. Norris, M.M. Shaker, F.K. Ko, Synth. Met. 114 (2000) 109.
[15] C.T. Hsieh, H. Teng, Carbon 40 (2002) 667.
[16] B.E. Conway, Electrochemical Supercapacitors, Kluwer Academic Publishers/Plenum Press, New York, 1999.